Chemical Science

ROYAL SOCIETY OF CHEMISTRY

EDGE ARTICLE

View Article Online
View Journal | View Issue

Cite this: *Chem. Sci.*, 2024, **15**, 6022

All publication charges for this article have been paid for by the Royal Society of Chemistry

Received 4th October 2023
Accepted 9th March 2024

DOI: 10.1039/d3sc05251f

rsc.li/chemical-science

Open shell (4*n* + 2)π and closed shell 4*n*π planar core-modified decaphyrins†‡

Pragati Shukla, Madan D. Ambhore and Venkataramanarao G. Anand *

Planar 44π and 46π core-modified decaphyrins with ten thiophene units have been synthesized from short thiophene oligomers. They have been structurally characterized by single crystal X-ray diffraction with further support from spectroscopic analysis and quantum chemical calculations. Our analysis revealed diradicaloid characteristics for 46π species in contrast to the closed shell property of the 44π congener. Further, 44π and 46π undergo reversible two-electron chemical oxidation, as observed by spectro-electrochemical measurements.

Introduction

Synthetic expanded porphyrinoids are excellent model systems to study Hückel, Möbius and Baird aromaticity.[1–4] Sustaining planarity in porphyrinoids containing forty or more π-electrons has remained a formidable challenge for synthetic chemists. Thermodynamic stability invariably favours non-planar topology at the expense of (anti)aromatic characteristics in π-expanded porphyrinoids. Sessler's tetracationic 40π decapyrrole, turcasarin, **1**, was the first giant porphyrinoid to be characterized with a figure-of-eight topology.[5] Subsequently, decaphyrins have regularly featured as non-planar macrocycles. For example, a decaphyrin, **2**, with ten pyrroles and ten bridging carbons also adopted a twisted topology.[6a,b] It is pertinent to note that a 40π octafuran and a 38π octaphyrins are the only large planar porphyrinoids known to display ring current effects.[7,8a,b] A couple of synthetic protocols have been explored to avoid a twisted topology by covalent/non-covalent support in the cavity of a decaphyrin. Osuka and co-workers attempted to induce a planar topology by covalently linking a phenylene ring in the centre of a redox-active 46π decaphyrin.[9] Later, Okujima and Kobayashi employed an anion template to synthesize a 38π dicationic cyclo[10]pyrrole through oxidative coupling of densely π-substituted bipyrrole.[10] Redox-active pyrrolic porphyrinoids with an identical number of heterocyclic units can be synthesized and isolated with different numbers of π-electrons in the macrocyclic network by varying: (a) the ratio between pyrrole units and bridging carbon atoms and (b) the number of imine/amine-like pyrrolic nitrogens.[11] Hence, (4*n* + 2)π pyrrolic decaphyrins are known to adopt between 46 and 38π electrons, while partially core-modified decaphyrins[12] vary between 48π and 40π electrons. Non-pyrrolic planar porphyrinoids display significantly altered electronic and redox properties compared to their corresponding pyrrole analogues, as reflected in their structural and electronic properties Fig. 1.[13]

A completely core-modified deca-thia decaphyrin, **3**, with a 1 : 1 ratio of thiophene and bridging carbons contains a maximum of 50π electrons and can be ring-oxidized to 48π dicationic species.[14] In the solid state, **3** can be tuned to adopt either a twisted (**3a**) or near-planar (**3b**) topology depending on

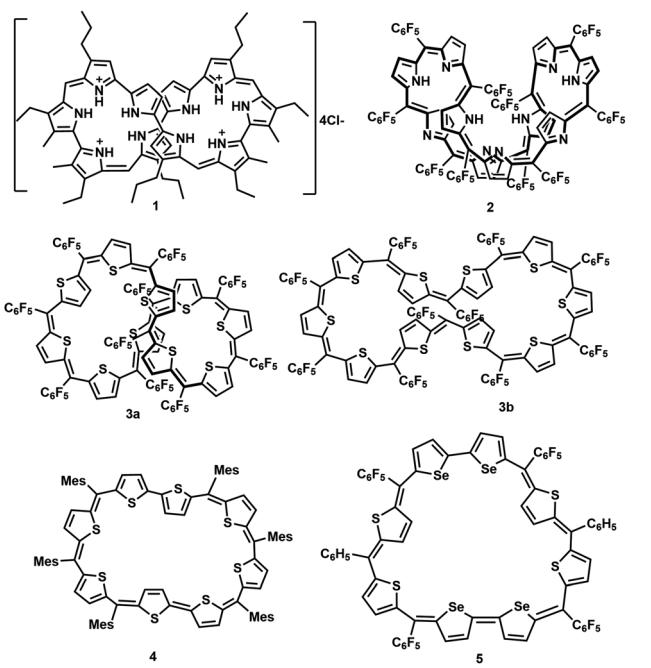

Fig. 1 Selected examples of expanded porphyrinoids with ten and eight heterocyclic units.

Department of Chemistry, Indian Institute of Science Education and Research (IISER), Pune 411008, Maharashtra, India. E-mail: vg.anand@iiserpune.ac.in

† Dedicated to Prof. Vadapalli Chandrasekhar on the occasion of his 65th birthday

‡ Electronic supplementary information (ESI) available. CCDC 2293502, 2294107, 2294108 and 2294163. For ESI and crystallographic data in CIF or other electronic format see DOI: https://doi.org/10.1039/d3sc05251f

the solvent of crystallization. Planar non-pyrrolic $(4n + 2)\pi$ octaphyrins, **4** and **5**, with bithiophene/biselenophene units display unique open shell configurations depending on the macrocyclic topology.[15,16a] In most known diradical species, such as linear oligothiophene or bisphenalenyls, an increase in the length of the spacer is known to increase the diradical character due to extra resonance energy attained by the diradicals.[16b] In this regard, it can be envisaged that a planar $(4n + 2)\pi$ decathiophene macrocycle could display pronounced diradicaloid features. Therefore, all the synthesized core-modified planar decaphyrins with varying number of π-electrons can be tested for their diradical properties. Herein, we report the first examples of planar 44π and 46π deca-thia porphyrinoids which display closed shell and open shell characteristics, respectively. Moreover, 42π dications of 44π macrocycles displayed moderate diradicaloid features.

Results and discussion

A synthetic strategy to induce a rigid planar structure for 50π decathiophene, **2**, can be envisaged by decreasing the number of bridging carbons in the macrocyclic framework. An attempt to synthesize a 44π decaphyrin was designed from short thiophene oligomers (See ESI,‡ for details of the synthesis). Acid-assisted condensation of terthiophene diol, **6**, with bithiophene, **7**, under dark and inert conditions in dichloromethane was followed by DDQ oxidation open to air (Scheme 1a). The MALDI-TOF/TOF mass spectrum of the reaction mixture revealed the formation of the expected 44π decathiophene, **10** (ESI S1‡). Under similar reaction conditions, the condensation of terthiophene diol **6** with either biselenophene, **8**, or bifuran, **9**, yielded 44π decaphyrins **11** and **12**, respectively (ESI S3 and S5‡). Encouraged by this success, we designed modified strategy (Scheme 1b) to synthesize a 46π decaphyrin, with six bridging carbons, by condensing terthiophene, **13**, with the diol of thia dipyrrane, **14**, under conditions similar to the synthesis of **10**. MALDI TOF/TOF mass spectral analysis of the reaction mixture (ESI S8‡) confirmed the identity of the target 46π decaphyrin, **15**.

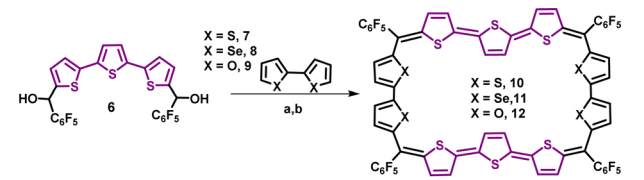

a. Synthesis of 44π decaphyrins **10**, **11** and **12**.

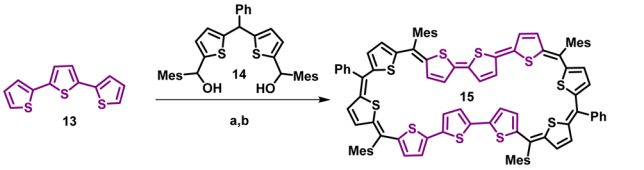

b. Synthesis of 46π decaphyrin **15**: (a) $BF_3.OEt_2$ (1 equiv.), dry CH_2Cl_2, 2 h, N_2 atmosphere, room temperature; (b) DDQ (3.5 equiv.), 2 h, open air conditions, room temperature.

Scheme 1 (a) Synthesis of 44π decaphyrins **10**, **11** and **12**. (b) Synthesis of 46π decaphyrin **15**: (a) BF_3 OEt_2 (1 equiv.), dry CH_2Cl_2, 2 h, N_2 atmosphere, room temperature; (b) DDQ (3.5 equiv.), 2 h, open air conditions, room temperature.

All the decaphyrins were isolated in 2.2 to 7.2% yields by column chromatography with dichloromethane and *n*-hexane as eluents. The absolute structure of these macrocycles was determined by ^{1}H NMR spectroscopy and single crystal X-ray diffraction studies. The ESI-TOF high resolution mass spectrum displayed an *m*/*z* value of 1535.8490 (calcd. for $C_{68}H_{20}F_{20}S_{20}$; $[M]^+$ 1535.8453) for **10** (ESI S2a‡), 1727.6244 (calcd. for $C_{68}H_{20}F_{20}S_6Se_4$; $[M]^+$ 1727.6231) for **11** (ESI S4‡), *m*/*z* value of 1471.9408 and 735.9665 (calcd. for $C_{68}H_{20}F_{20}O_4S_6$; $[M]^+$ 1471.9366 and $[M]^{2+}$ 735.9683) for **12** (ESI S6‡) and *m*/*z* value of 761.1470 (calcd. for $C_{94}H_{74}S_{10}$; $[M]^+$ 1522.2998 and $[M]^{2+}$ 761.1499) for **15** (ESI S9‡). The proton NMR spectrum of decathiophene **10** recorded in $CDCl_3$ displayed well-resolved signals at room temperature. A sharp singlet at δ 8.69 ppm and four distinct doublets at δ 6.58, 6.55, 6.09 and 5.87 ppm corresponding to four protons each (ESI S11‡) were observed. The ^{1}H–^{1}H two-dimensional NMR spectrum revealed two sets of correlations for doublets (δ 6.58, 6.09 ppm and δ 6.55, 5.87 ppm) in support of the coupling of β-CH protons of thiophene rings (ESI S12‡). A lower number of signals suggested higher symmetry for the macrocycle in the solution state. A similar ^{1}H NMR spectral pattern at room temperature in $CDCl_3$ was observed for tetra-selena derivative, **11**, with five signals in the region between δ 6.04 and 8.41 ppm (ESI S13‡). Tetraoxa derivative, **12**, also displayed a similar well-resolved spectrum with relatively downfield chemical shift values between δ 6.80 and 7.53 ppm (ESI S14‡).

The absolute molecular structure of **10** was determined by X-ray diffraction of single crystals obtained by vapor diffusion of *n*-hexane into its solution in chloroform. **10** adopted a squarish arrangement with all the thiophene rings in same plane and *meso*-pentafluoro substituents oriented almost perpendicular to the macrocyclic plane defined by four bridging carbons. The central thiophene in both the terthiophene units was inverted with its sulfur atom facing away from the macrocyclic core (Fig. 2a and b). Such a symmetrical molecular structure is in good agreement with the observed ^{1}H NMR spectrum of **10**. Further, the value +5.93 ppm for the estimated nucleus-independent chemical shift (NICS)[17] calculated at the B3LYP/6-31G(d,p) level of theory suggested poor antiaromatic character for the 44π macrocycle. Similar to **10**, the tetra-oxa derivative **12**, also displayed a near-planar structure in the solid state (Fig. 2c and d). Unexpectedly, it revealed inversion of two adjacent thiophene rings in each of the terthiophene units with symmetry much lower than that of decaphyrin **10**. This conformation is perhaps more pronounced in the solid state and may not correspond to the solution state structure as analyzed from its ^{1}H NMR spectral features. Earlier reports revealed that it is not uncommon for expanded porphyrinoids to adopt different structures in solid and liquid states.[9,16a] The molecular structure of 46π decaphyrin **15** determined from X-ray diffraction studies revealed a planar and rectangular topology. Two adjacent thiophene rings were inverted in each

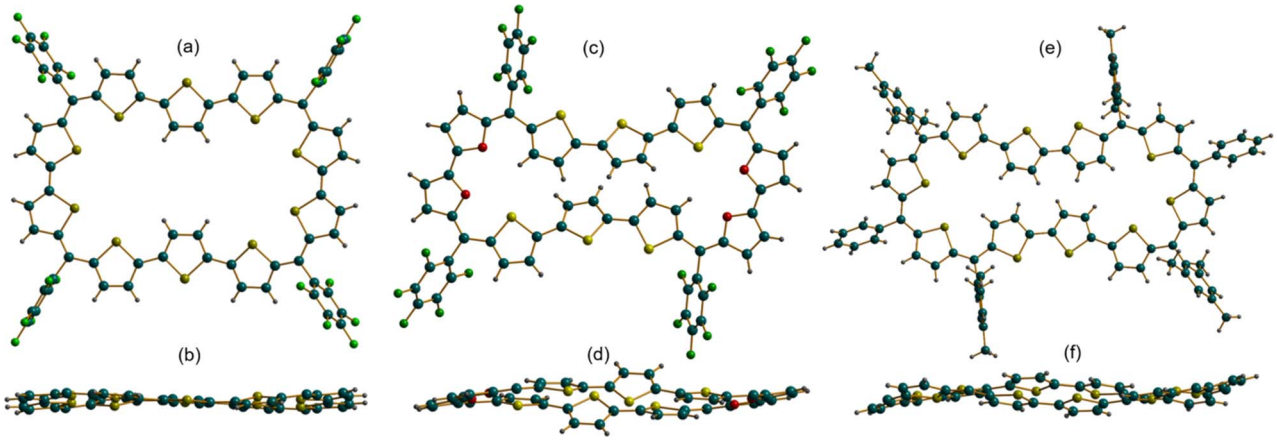

Fig. 2 Molecular structure of decaphyrins **10** (a and b), **12** (c and d) and **15** (e and f) with side view and top view. Images a, c and e represent the top view while images b, d and f represent the side view, where *meso*-substituents are omitted for clarity.

terthiophene, while the sulfur atoms of the other six thiophene rings are oriented towards the macrocyclic core (Fig. 2e and f). To the best of our knowledge, these are the largest planar porphyrinoids known to date. Being a planar and globally π-conjugated structure comprising 46 π-electrons, it adheres to Hückel's aromatic structure. An estimated NICS value of −17.94 ppm at the macrocyclic centre further substantiated Hückel aromaticity for the 46π macrocycle (ESI S33b‡). A clockwise direction of ring current in **15** obtained from the plot of computed anisotropy of induced current density (ACID)[18] further supports the aromatic character in this $(4n + 2)\pi$ macrocycle. However, the ACID plot for **10** did not reveal an exclusive direction of the ring current in tune with the estimated NICS value (ESI S31 and S32‡). In addition, the computationally calculated harmonic oscillator model of aromaticity (HOMA)[19a] values of 0.74 and 0.88 for **10** and **15** corroborate respective aromatic characteristics for these π circuits. The estimated values for the electronic aromaticity indices AV_{1245} and AV_{min}[19b,c] (for **10**) are 1.68 and 1.00, respectively, and relatively higher values of 2.84 and 1.78 were obtained for **15**. Thus, comparable increases in the index values for **15** suggest the aromatic characteristics of the 46π decaphyrin.

In stark contrast to structural and computational studies, 46π decaphyrin **15** did not display well resolved signals in its ^{1}H NMR at room temperature. Suspecting its fluxional nature, we recorded ^{1}H NMR spectra at lower temperatures up to 198 K (ESI S18‡), which revealed only broad signals in the region between δ 6.00 and 9.00 ppm supporting diradicaloid characteristics for the planar 46π macrocycle. Our earlier reports suggest that such $(4n + 2)\pi$ systems with relatively broad ^{1}H NMR signals signify the diradicaloid character of the macrocycle.[15,16a] To further confirm the diradicaloid properties of **15**, variable-temperature EPR was recorded, and it displayed a broad signal with a *g* value of 2.0054. The EPR signal intensity decreases with a decrease in temperature, suggesting a singlet ground state (Fig. 3a). To support experimental findings, quantum chemical calculations using the UCAM-B3LYP/6-31G(d,p) method revealed a singlet–triplet energy gap ΔE_{S-T} of −2.19 kcal mol^{-1}. Moreover, it yielded an occupation number NOON (natural orbital occupation number)[20] of 0.84 for the LUMO and a y_0 value of 0.69, suggesting a diradicaloid character (ESI Table S1a‡). The obtained NOON value for decathiophene is much higher than that reported for 38π octathiophene,[15,16a] which is close to 0.40% with an occupation number of 0.67 for the LUMO. The frontier molecular orbital diagram (FMO) shows the electron density of two electrons localised over two halves of conjugated macrocycle **15** (Fig. 4). It can be envisaged that the quinoidal form **15a** is fully conjugated and is in resonance with the benzenoidal form **15b** of the macrocycle corresponding to the open shell conformation (Fig. 3b). Its additional stability can be attributed to the increased number of aromatic thiophene rings of the terthiophene moiety in the planar topology. However, antiaromatic 44π decathiophene, **10**, did not display any diradicaloid features, as analyzed in experimental and computational studies (ESI Table S2‡). Various basis sets have been employed for determining the aromatic characteristics of poly-aromatic hydrocarbons and porphyrin-based systems.[21] However, our calculations with B3LYP/6-31G(d,p) level of theory

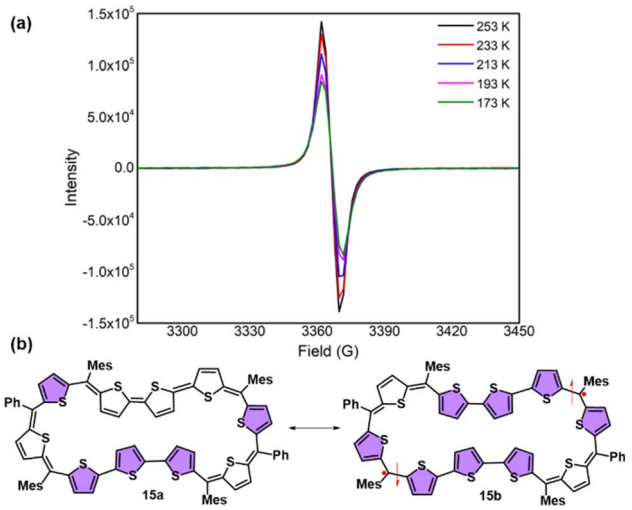

Fig. 3 (a) Variable-temperature EPR spectra of **15**. (b) Fully conjugated form **15a** and diradicaloid form **15b** of decaphyrin **15**.

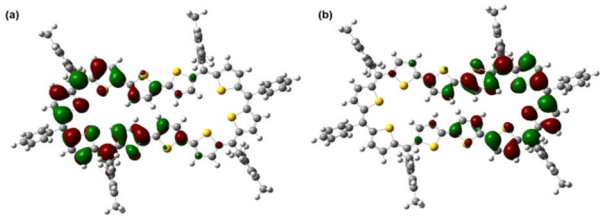

Fig. 4 Frontier SOMO profiles, calculated using spin-unrestricted UCAM-B3LYP/6-31G(d,p) for **15**: (a) SOMO α spin and (b) SOMO β spin.

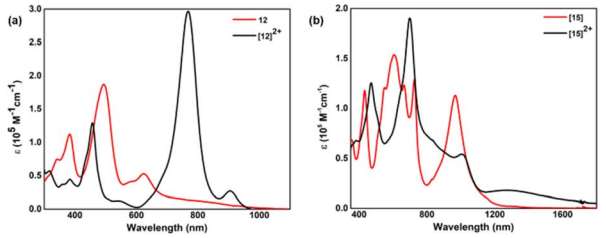

Fig. 5 UV-visible absorption spectra of (a) **12** and $[\mathbf{12}]^{2+}$, (b) **15** and $[\mathbf{15}]^{2+}$.

matched the observed experimental results. The diradicaloid character was estimated with the UCAM B3LYP/6-31G(d,p) basis set.

By virtue of extended π-conjugation, 44π decaphyrin, **10**, displayed strong absorptions at 507 (136 500) and 602 (185 000) nm (ESI S23‡). Tetra-selena derivative **11** also displayed similar absorptions, while the tetra-oxa derivative **12** displayed strong absorption (Fig. 5a) at 494 (187 000) nm and relatively weak bands at 384 (112 400), 583 (41 200) and 624 (52 900) nm. In contrast, 46π decaphyrin, **15**, displayed multiple absorptions (Fig. 5b) at 432 (117 800), 546 (sh), 605 (153 800), 664 (sh) and 725 (128 700) nm. A relatively intense and broad absorption band at 966 (112 900) nm extending to NIR supports the diradicaloid nature of **15** (Table 1). Such wide-ranging absorptions in the visible part of the electromagnetic spectrum are uncommon in giant porphyrinoids.

Since $4n\pi$ porphyrinoids are susceptible to reversible two-electron ring oxidation,[13] the redox property of 44π decaphyrins was studied by chemical and spectro-electrochemical methods. The 44π decaphyrins **10–12** could be reversibly oxidized to their respective 42π dicationic species, by various reagents such as trifluoroacetic acid, $[Et_3O]^+[SbCl_6]^-$, $NOBF_4$, $NOSbF_6$ or triflic acid (Scheme 2). Upon oxidation, a subtle change from a purple to bluish color along with intense red-shifted absorptions at 772 nm (450 800) nm were observed for

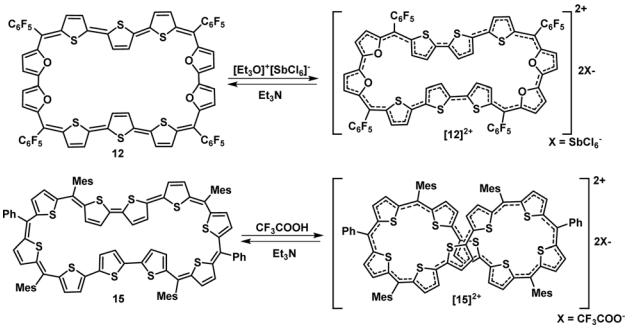

Scheme 2 Oxidation of **12** and **15** to their corresponding dications $[\mathbf{12}]^{2+}$ and $[\mathbf{15}]^{2+}$.

$[\mathbf{10}]^{2+}$ (ESI S23‡). Unfortunately, dications were less stable in common organic solvents over a period of time and hence eluded their complete characterization. Hence, we could not successfully grow single crystals to determine their absolute structure. However, dicationic $[\mathbf{10}]^{2+}$ ($m/2$) species could be identified from the HR-MS spectrum to confirm the ring oxidation of the macrocycle (ESI S2b‡). Since dication $[\mathbf{10}]^{2+}$ is a Hückel $(4n + 2)\pi$ aromatic system, we suspected it to exhibit a diradicaloid feature in its planar conformation. Hence, computational studies for $[\mathbf{10}]^{2+}$ were performed with similar parameters to those employed for **15**. As anticipated, it displayed a singlet triplet energy gap ΔE_{S-T} of −2.61 kcal mol^{-1}. These values suggested a thermally accessible triplet state, and it also had a NOON value of $y_0 = 0.50$ displaying a moderately diradicaloid character (ESI Table S2‡). These results are in further support of our findings of a significant increase in diradicaloid character with increasing length of π-conjugation in aromatic expanded porphyrinoids. Analogous color changes and red-shifted absorptions were observed upon oxidation of the tetra-selena and tetra-oxa 44π decaphyrins **11** and **12**. $[\mathbf{12}]^{2+}$ displayed intense red-shifted absorptions at 768 (296 000) and 457 (129 400) nm, which were associated with a color change from brownish-green to yellowish-green upon oxidation.

Cyclic voltammetry studies revealed four oxidations at 0.40, 0.75, 1.08 and 1.35 V and one reduction at −0.88 V for the 44π macrocycle **12** (ESI S27‡). Spectro-electrochemical measurements (ESI S29‡) also revealed an absorption at 768 nm at an applied potential of 0.87 V validating dicationic species derived upon chemical oxidation by a Meerwein salt.[22] Fortunately, the tetra-oxa decaphyrin $[\mathbf{12}]^{2+}$ could be isolated and characterized by ^{1}H NMR spectroscopy. It displayed a well-resolved spectrum with ten doublets in the region between δ 4.0 and 9.00 ppm (ESI S16‡) at room temperature. The number of resonances was

Table 1 Decaphyrins with their electronic absorption values

Decaphyrin	No. of πe^-	λ_{max} (nm) ε (M^{-1} cm^{-1})
10	44	507 (136 500), 559 (80 500) and 602 (185 000)
11	44	505 (94 900), 547 (63 700) and 589 (124 700)
12	44	384 (112 400), 494 (187 000), 583 (41 200) and 624(52 900)
15	46	432 (117 800), 546 (sh), 605 (153 800), 664 (sh), 725 (128 700) and 966 (112 900)

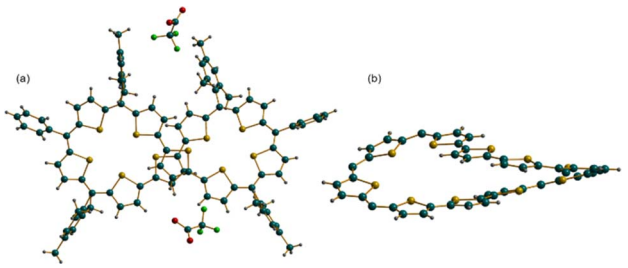

Fig. 6 Molecular structure obtained from an X-ray diffraction study of decaphyrin dication $[\mathbf{15}]^{2+}\cdot 2(CF_3COO)^-$: (a) side view and (b) top view.

twice the number observed in its freebase form. The ^{1}H–^{1}H COSY spectrum (ESI S17‡) revealed five correlations, suggesting inversion of two adjacent thiophene rings in both the terthiophene units, as observed from X-ray diffraction studies of the parent macrocycle. Its estimated NICS value of −17.82 ppm further supported the aromaticity of 42π dication $[\mathbf{12}]^{2+}$. All our efforts to crystallize $(4n + 2)\pi$ dicationic species $[\mathbf{12}]^{2+}$ were futile.

Similar two-electron ring oxidation was also observed for 46π diradicaloid decaphyrin, **15** (Scheme 2). Upon addition of a Meerwein salt or TFA, intense red-shifted absorptions were observed at 470 (125 200), 698 (190 100) and 1008 (54 000) nm for 44π dicationic species, $[\mathbf{15}]^{2+}$. Two-electron ring oxidation for the $(4n + 2)\pi$ species was further supported by the observation of the $m/2$ value from high resolution mass spectrometry (ESI S10‡) and from spectro-electrochemical studies (ESI S30‡). The ^{1}H NMR spectrum of $[\mathbf{15}]^{2+}$ revealed only broad signals at room temperature. However, in contrast to 46π species, the 44π dication species $[\mathbf{15}]^{2+}$ displayed sharp resonances upon lowering the temperature to 203 K (ESI S21‡). Ten resonances were observed within a small region between δ 6.75 and 8.12 ppm, resulting in the overlap of many signals. Methyl protons of mesityl rings were found to resonate between δ 1.41 and 2.99 ppm. These chemical shift values did not reflect the paratropic ring current effect expected of planar $4n\pi$ species.

Crystallization of $[\mathbf{15}]^{2+}$ was attempted with various solvent systems, and the best possible crystals were obtained by vapor diffusion of heptane into a solution of $[\mathbf{15}]^{2+}$ in dichloromethane. The molecular structure of 44π dication $[\mathbf{15}]^{2+}\cdot 2(CF_3COO)^-$ obtained from X-ray diffraction analysis revealed a twisted conformation, resulting in the loss of the anticipated antiaromatic character. The dicationic nature of the figure-of-eight conformation was confirmed by two associated CF_3COO^- counter-anions for the dipositive charge on the macrocycle (Fig. 6). This structure also represents an unusual criss-crossing of the two terthiophene units in the centre of the macrocycle forming two five-membered pockets. Structure-induced loss of antiaromaticity led to a closed shell 44π species, which could be reduced back to the parent planar 46π macrocycle with appropriate reducing agents such as triethylamine or Zn dust. Even the 42π dication of decaphyrins **12** could be reduced back to the parent 44π macrocycle with similar reducing agents.

Conclusions

We have described novel examples of planar decaphyrins bearing 44π and 46π electrons. Their structural characterization was accomplished by X-ray diffraction studies and spectroscopic investigations. Our analyses reveal that a planar $(4n + 2)\pi$ species is stabilized as a diradicaloid, and such macrocyclic character can be enhanced by extending the length of conjugation, while the 44π species adopts a closed shell configuration with a flat topology. Both species undergo reversible two-electron ring oxidation to yield the corresponding 42π and 44π dicationic species. Electrochemical studies suggest multiple oxidation states which have yet to be accessed by appropriate chemical reagents. Significantly, these studies suggest that accommodating short thiophene oligomers in planar $(4n + 2)\pi$ electron giant porphyrinoids may have a greater tendency to adopt radicaloid characteristics to sustain aromaticity. The synthesis of such giant porphyrinoids is underway in this laboratory.

Data availability

Details of synthesis, spectroscopic characterization, co-ordinates obtained from computational calculations and CCDC numbers for the molecular structures are made available in ESI.‡

Author contributions

P. S. contributed to syntheses, spectroscopic characterizations, X-ray data, computational calculations and assisted in writing the manuscript. M. D. A. was involved in synthetic design and computational calculations. V. G. A. conceptualized and managed the whole project and wrote the manuscript.

Conflicts of interest

There are no conflicts to declare.

Acknowledgements

VGA thanks Department of Science and Technology (DST), New Delhi, India, for the Swarnajayanti Fellowship and SERB (Grant no: CRG/2019/005046), New Delhi, India for the financial support. PS and MDA thank Indian Institute of Science Education and Research (IISER), Pune, India, for their respective research fellowships. Authors acknowledge DST-FIST, New Delhi, India, grant (SR/FST/CS-II/2019/105) for the VT EPR facility at IISER Pune, India. Authors acknowledge IISER Pune, India, for the high performance computating cluster facility for the quantum chemical calculations.

References

1 D. Seidel and J. L. Sessler, *Angew. Chem., Int. Ed.*, 2003, **42**, 5134–5175.
2 T. Tanaka and A. Osuka, *Chem. Rev.*, 2017, **117**, 2584–2640.

3 M. Stepien, N. Sprutta, P. Chwalisz, L. Szterenberg and L. L. Grazynski, *Angew. Chem., Int. Ed.*, 2007, **46**, 7869–7873.
4 S. Venkatraman and T. K. Chandrashekar, *Acc. Chem. Res.*, 2003, **36**, 676–691.
5 J. L. Sessler, S. J. Weghorn, V. Lynch and M. R. Johnson, *Angew Chem. Int. Ed. Engl.*, 1994, **33**, 1509–1511.
6 (*a*) S. Shimizu, N. Aratani and A. Osuka, *Chem.–Eur. J.*, 2006, **12**, 4909–4918; (*b*) Y. Tanaka, J.-Y. Shin and A. Osuka, *Eur. J. Org Chem.*, 2008, 1341–1349.
7 J. S. Reddy, S. Mandal and V. G. Anand, *Org. Lett.*, 2006, **8**(24), 5541–5543.
8 (*a*) W. Y. Cha, T. Soya, T. Tanaka, H. Mori, Y. Hong, S. Lee, K. H. Park, A. Osuka and D. Kim, *Chem. Commun.*, 2016, **52**, 6076–6078; (*b*) M. D. Ambhore, A. Basavarajappa and V. G. Anand, *Chem. Commun.*, 2019, **55**, 6763–6766.
9 V. G. Anand, S. Saito, S. Shimizu and A. Osuka, *Angew. Chem., Int. Ed.*, 2005, **44**, 7244–7248.
10 T. Okujima, C. Ando, S. Agrawal, H. Matsumoto, S. Mori, K. Ohara, I. Hisaki, T. Nakae, M. Takase, H. Uno and N. Kobayashi, *J. Am. Chem. Soc.*, 2016, **138**, 7540–7543.
11 M. Broring, J. Jendrny, L. Zander, H. Schmickler, J. Lex, Y. D. Wu, M. Nendel, J. Chen, D. A. Plattner, K. N. Houk and E. Vogel, *Angew Chem. Int. Ed. Engl.*, 1995, **34**, 2515–2516.
12 A. Ghosh, S. Dash, A. Srinivasan, C. H. Suresh, S. Peruncheralathan and T. K. Chandrashekar, *Org. Chem. Front.*, 2019, **6**, 3746–3753.
13 B. K. Reddy, A. Basavarajappa, M. D. Ambhore and V. G. Anand, *Chem. Rev.*, 2017, **117**, 3420–3443.
14 H. S. Udaya, A. K. Basavarajappa, T. Y. Gopalakrishna and V. G. Anand, *Chem. Commun.*, 2022, **58**, 13931–13934.
15 Y. Ni, T. Y. Gopalakrishna, S. Wu and J. Wu, *Angew. Chem., Int. Ed.*, 2020, **59**, 7414–7418.
16 (*a*) M. D. Ambhore, P. Shukla, R. G. Gonnade and V. G. Anand, *Chem. Commun.*, 2022, **58**, 8946–8949; (*b*) Z. Zeng, X. Shi, C. Chi, J. T. Lopez Navarrete, J. Casado and J. Wu, *Chem. Soc. Rev.*, 2015, **44**, 6578–6596.
17 P. V. R. Schleyer, C. Maerker, A. Dransfeld, H. Jiao and N. J. R. van Eikema Hommes, *J. Am. Chem. Soc.*, 1996, **118**, 6317–6318.
18 D. Geuenich, K. Hess, F. Kohler and R. Herges, *Chem. Rev.*, 2005, **105**, 3758–3772.
19 (*a*) T. M. Krygowski and M. K. Cyranski, *Chem. Rev.*, 2001, **101**, 1385–1420; (*b*) E. Matito, *Phys. Chem. Chem. Phys.*, 2016, **18**, 11839–11846; (*c*) I. C. Reig, T. Woller, J. C. Garcıa, M. Alonso, M. T. Sucarrat and E. Matito, *Phys. Chem. Chem. Phys.*, 2018, **20**, 2787–2796.
20 D. Dohnert and J. Koutecky, *J. Am. Chem. Soc.*, 1980, **102**, 1789–1796.
21 (*a*) I. C. Reig, E. R. Cordoba, M. T. Sucarrat and E. Matito, *Molecules*, 2020, **25**, 711; (*b*) I. C. Reig, R. G. Aviles, E. R. Cordoba, M. T. Sucarrat and E. Matito, *Angew. Chem., Int. Ed.*, 2021, **60**, 24080–24088; (*c*) J. Wu, *Diradicaloids*, Jenny Stanford Publishing, 2022.
22 R. Rathore, A. S. Kumar, S. V. Lindeman and J. K. Kochi, *J. Org. Chem.*, 1998, **63**, 5847–6682.